

**A W G N**

**DC - offset**

**A Study on a Elimination Method of DC - offset in Direct - Conversion  
Receiver under Additive White Gaussian Noise Environment**

**2000 8**

本 論 文

工 學 碩 士 學 位 論 文

認 准 .

:

:

:

2001 2

Nomenclature

Abstract

1	.....	1
2	Direct-conversion	..... 4
2-1.	Heterodyne Direct-conversion	..... 4
2-2.	Direct-conversion	..... 12
2-3.	Direct-conversion	..... 19
3	DC-offset	..... 21
3-1.	DC-offset	..... 21
3-2.	DC-offset	..... 25
3-3.	AWGN	..... 29
4	DC-offset	..... 33
4-1.		..... 34
4-2.	AC-coupling	..... 36
4-3.	DC-feedback DC-offset	..... 37
5		..... 40
5-1.	QPSK	..... 40
5-2.	QPSK	..... 42
5-3.		..... 44
6	.....	46
	.....	48

## Nomenclature

- $F_{LNA}$  : Noise Figure of LNA  
 $F_{mix}$  : Noise Figure of mixer  
 $f_{lpf}$  : Cutoff-frequency of filter  
 $G_{LNA}$  : Gain of LNA  
 $G_{mix}$  : Gain of mixer  
 $O_{lpf}$  : Order of filter  
 $R_{dc}$  : Amplitude of dc due to paracitic coupling  
 $r$  : Rolloff factor  
 $\Delta f$  : Doppler shift frequency  
 $\xi^3_{dsr}$  : Ratio of Power about DC-offset  
 $\phi_{dc}$  : Phase of DC  
 $\phi(t)$  : Phase distortion in signal due to ISI  
 $\eta(t)$  : Phase distortion due to AWGN  
 $\theta_{dc}$  : Error of DC-offset  
 $\omega_c$  : Carrier frequency

## **Abstract**

Recently, the performance of the commercial PCS (Personal Communication Service) system has been improved to the uppermost limit and ultimately the next generation mobile communication is to be realized by IMT-2000 (International Mobile Communication-2000) to provide multimedia services.

Therefore, the new type receiving system is researched actively and one of the most important part in a receiver is direct conversion method. The direct conversion method is suitable for low power consumption, small size, MMIC, and low price, which is to be adopted to the next generation mobile communication systems. In this case, however, several problems occur due to DC-offset. The DC-offset suppresses amplification of the required signal because of the leakage signal of frequency synthesizer in the system.

In this thesis, the removing method of DC-offset was considered. There are four removing techniques of DC-offset, which are AC-coupling, large capacitor, dc-feedback loop, and dc-free coding. Among these, the AC-coupling method is the most simplest method and the dc-feedback loop method has the best performance. Then, the performance of the AC-coupling method and dc-feedback loop method are evaluated by HP's ADS simulation tool.

As a result, the AC-coupling method cannot be used to the digital communication systems due to data loss. On the other hand, it was confirmed that the dc-feedback loop method is suitable for the direct conversion receiver.



(Direct-conversion) .  
 Direct-conversion 1940 ,  
 가  
 . ,  
 Direct-conversion  
 . Direct-conversion  
 가 , 가  
 . RF  
 , IF , (Image rejection  
 filter) . , 가 SAW filter ,  
 (Low pass filter) (Amplifier) 가 가 가  
 가 . 40%  
 가 . , 2  
 가 ,  
 가 . , Direct-conversion  
 ,  
 . , 가 filter RF  
 (One-Chip)가 가 . , Direct-  
 conversion 가  
 가 가 . 가  
 DC(Direct Current)-offset . DC-offset  
 , DC-offset  
 BER .  
 DC-offset , Direct-conversion  
 . DC-offset 가  
 . Direct-conversion  
 QPSK (Quadrature Phase Shift Keying)

, . , , ,  
 . , Direct-conversion  
 DC-offset AC-coupling DC-feedback  
 ,  
 2 Direct-  
 conversion ,  
 Direct-conversion . 3 Direct-  
 conversion DC-offset . DC-  
 offset AWGN BER  
 , 4 AC-coupling  
 , AC-coupling  
 DC-feedback  
 . 5  
 IMT-2000 .  
 HP ADS (Advanced Design Systems)  
 . 6  
 Direct-conversion .

## 2 Direct-Conversion

Heterodyne

Direct-Conversion

### 2-1. Heterodyne

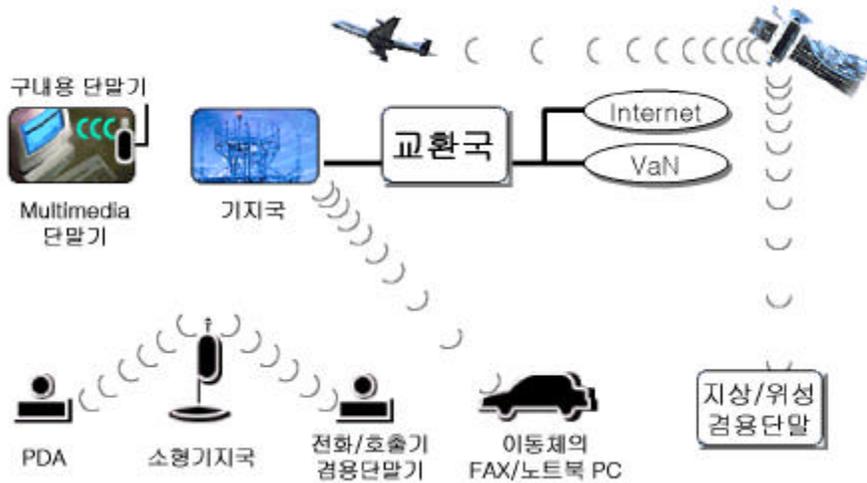
### Direct-Conversion

IMT-2000

가

IMT-2000

가



2-1 IMT-2000

Fig. 2-1 IMT-2000 Service Concept Diagram.

2-1 IMT-2000  
 . ITU-R 1999 ,  
 가 ,  
 IMT-2000

2-1

Table 2-1 Technology current of the global.

	2	3
	CDMA	2 CDMA , CDG
	PDC PHS	IMT-2000 NTT DoCoMo
	GSM	GSM

2-2

Table 2-2

3GPP2( )	ANSI-41 , CDMA2000
3GPP( )	GSM-MAP , W-CDMA
OHG( )	/ 가 module

2-1

2-2

IMT-2000

Direct-conversion

RF

IF

,

(40% )

RF

가

가

가

.

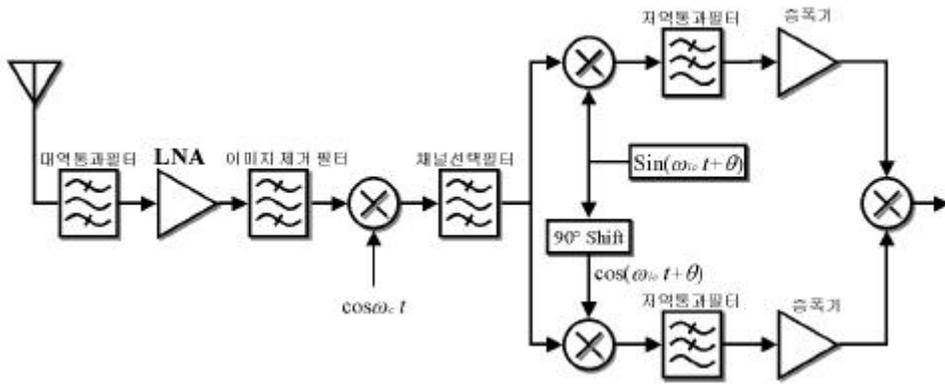
가

.

## 2-1-1 Superheterodyne

1918 Armstrong  
(selectivity)  
98%가

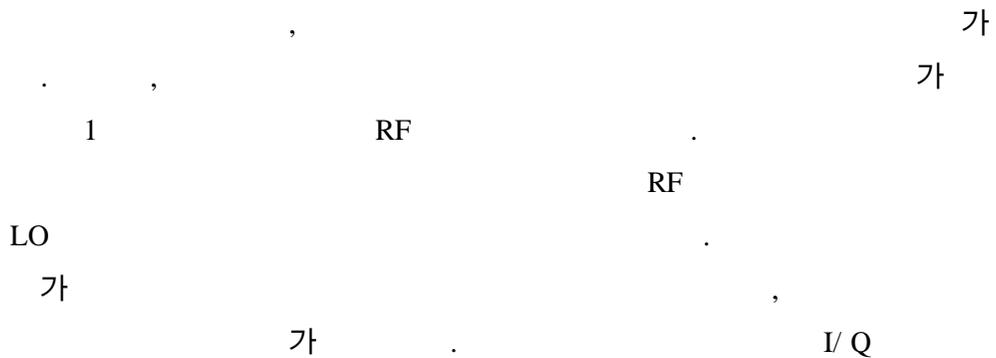
Heterodyne  
(sensitivity) 가

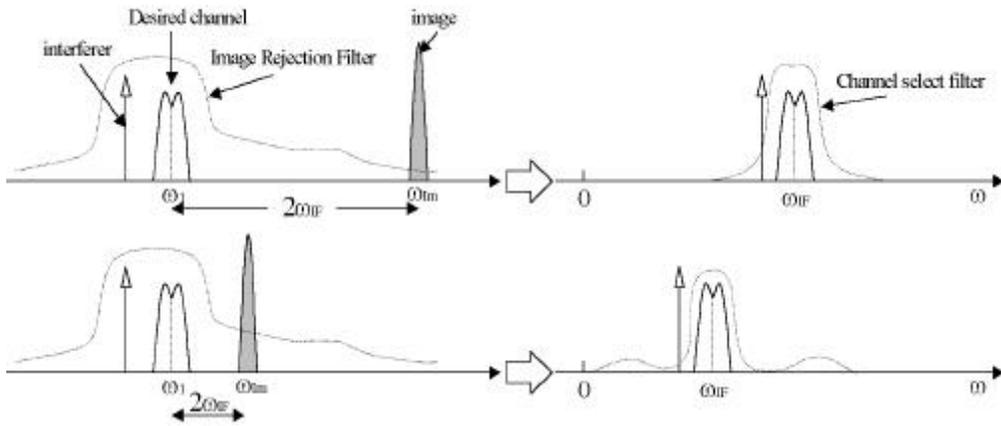


## 2-2 Quadrature heterodyne

Fig. 2-2 Heterodyne receiver architecture with quadrature.

## 2-2 Quadrature Heterodyne





2-3

Fig. 2-3 Image Frequency Remove using Image Rejection Filter.

Heterodyne

2-3

$$\omega_1 (= \omega_{LO} - \omega_{IF})$$

$$\omega_{im} (= \omega_{LO} + \omega_{IF})$$

가

$$2\omega_{IF}$$

Heterodyne

Q

가

가

가

IF

가

IC

SAW filter

bulky filter

가

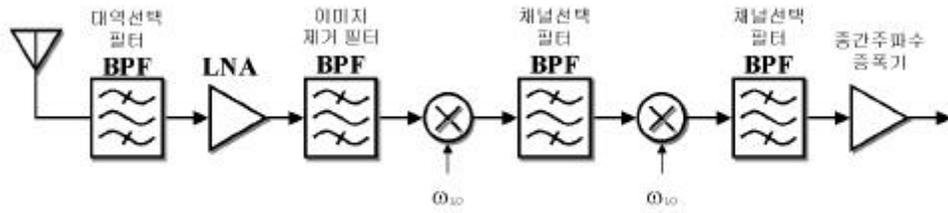
system

rejection

IF

2-4

2



2-4 2

Heterodyne

Fig. 2-4 2nd step Downconversion Heterodyne Receiver.

Heterodyne

가

가

50

trade-off

### 2-1-2. Direct-Conversion

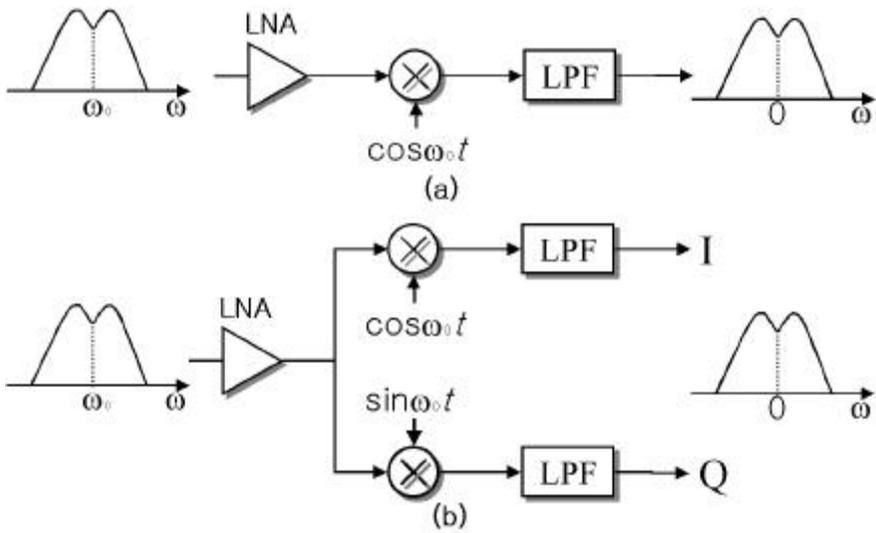
Direct-conversion

Heterodyne

RF

LO(Local Oscillator)

0 Hz



2-5 Direct-conversion (a) (b)

Fig. 2-5 Direct-Conversion Architecture (a) with Simply (b) with Quadrature

2-5(a)

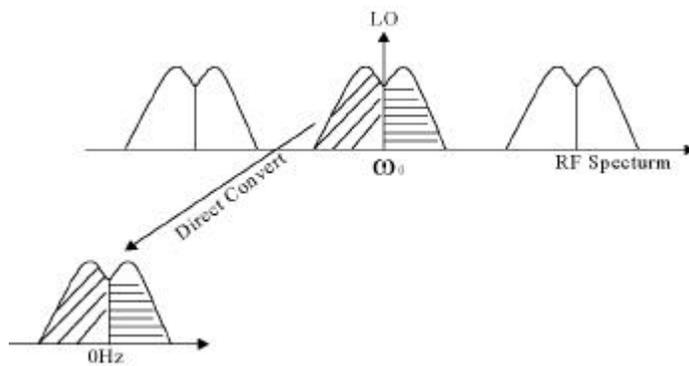
가

Double-sideband

2-5(b)

FM

QPSK



2-6 Direct-conversion

Fig. 2-6 Spectrum before and after Direct-Conversion.

2-6 Direct-conversion

conversion

가 Direct-

Heterodyne

RF preselect filter

가

Direct-conversion

, LO

가

**Homodyne**

## 2-2. Direct-Conversion

### 2-2-1. Direct-Conversion

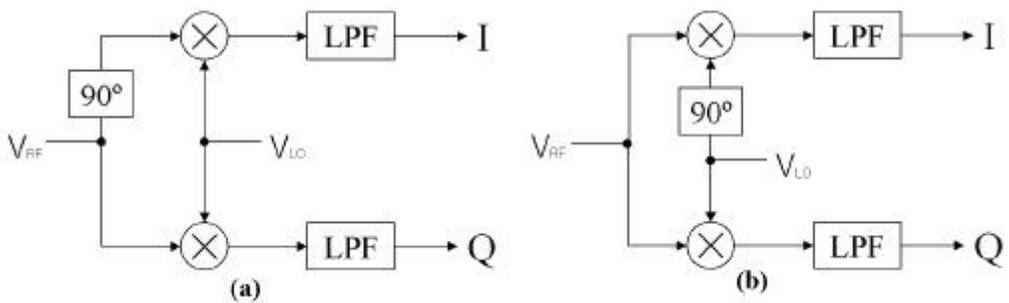
- Direct-conversion Heterodyne 가
- (1) IF가 0 Hz , .
- (2) 가 가 50 load  
가 .
- (3) Heterodyne IF SAW filter 가  
,  
IC system .
- (4) Heterodyne 가 . 가

### 2-2-2. Direct-Conversion

- Direct-conversion Heterodyne  
0 Hz Heterodyne  
가 .  
DCR (Direct-conversion receiver) 가  
DC-offset, I/ Q mismatch, even-order distortion .
- DC-offset
- DC-offset 가 , offset offset  
. offset process mismatch

drift, offset LO RF , DCR , DCR DC-offset 가 . 3 .

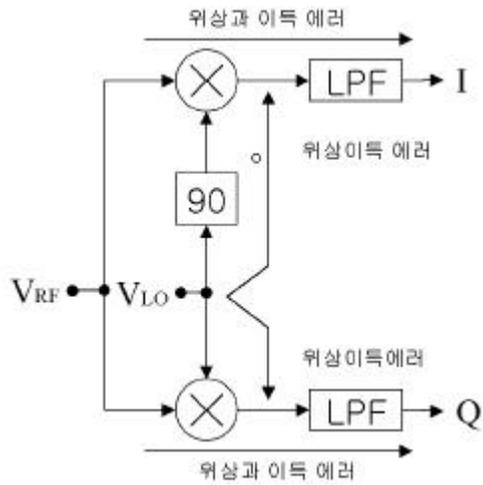
I/Q Mismatch



2-7 Quadrature (a) RF (b) LO

Fig. 2-7 Quadrature generation in (a) RF path. (b) LO path.

2-7 DCR quadrature LO RF 가 90° 가 RF - trade-off 2-7(b) LO 90° I Q error . I, Q .



2-8 IQ

Fig. 2-8 IQ Mismatch.

2-8 I/Q

I/Q

가

$$x_{in}(t) = a \cos \omega_c t + b \sin \omega_c t \quad [a, b = \pm 1] \quad (2-1)$$

LO

I Q

가

$$\left. \begin{aligned} x_{LO,I}(t) &= 2 \cos \omega_c t \\ x_{LO,Q}(t) &= 2(1 + \varepsilon) \sin(\omega_c t + \theta) \end{aligned} \right\} \quad (2-2)$$

( $\varepsilon$  :           ,  $\theta$  :           )

(2-1)  $x_{in}(t)$  LO ,

$$\left. \begin{aligned} x_{BB,I}(t) &= a \\ x_{BB,Q}(t) &= (1 + \varepsilon)b \cos \theta - (1 + \varepsilon)a \sin \theta \end{aligned} \right\} \quad (2-3)$$

constellation 2-9 signal

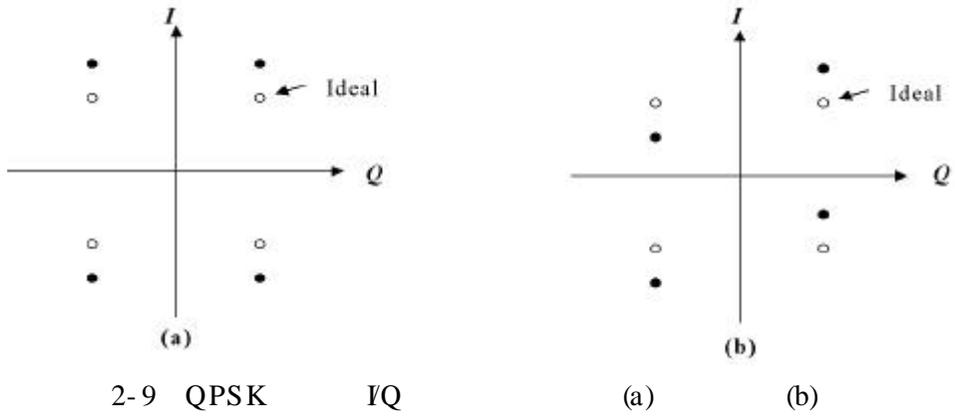


Fig.2-9 IQ mismatch effect of QPSK signal (a) Gain error(b) Phase error.

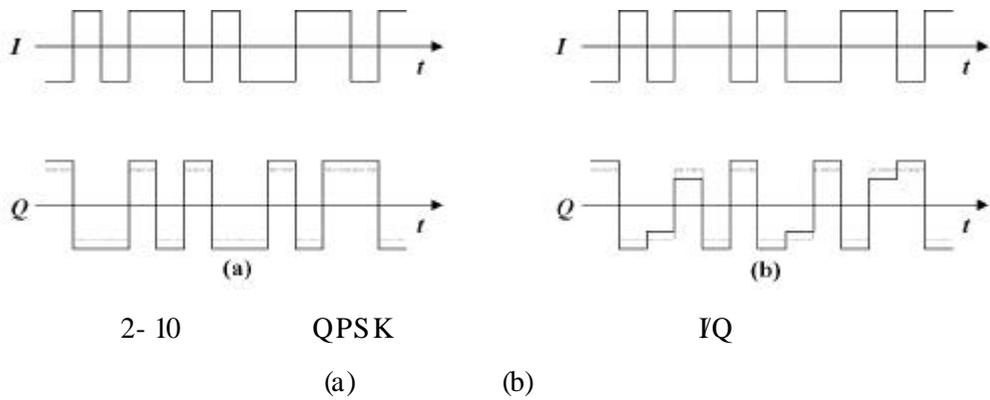


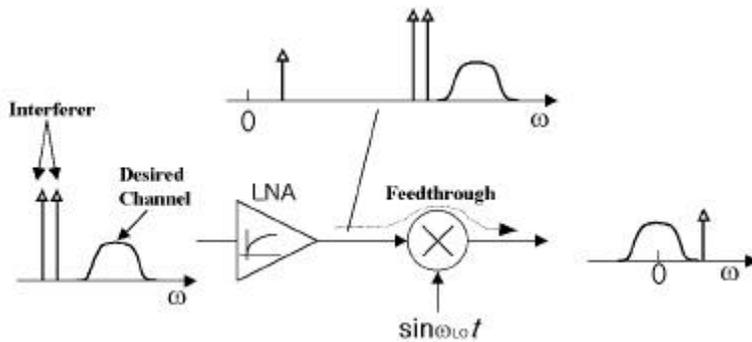
Fig.2-10 IQ mismatch effect of demodulated QPSK signal in time domain.  
(a) Gain error. (b) Phase error.

2-10

I/Q data

ratio) , I/Q bit data SNR(Signal to Noise ratio) . data pulse 가 I, Q data stream 가 SNR Heterodyne , Homodyne / 가 가 . 가 Homodyne Heterodyne I/Q 50 dB 60 dB 가 / Heterodyne I/Q IC , Homodyne 가 MMIC

Even-Order Distortion



2- 11

Fig. 2- 11 Effect of even-order distortion on interferers.

$$y(t) = \alpha_1 x(t) + \alpha_2 x^2(t) \tag{2-4}$$

$$x(t) = A_1 \cos \omega_1 t + A_2 \cos \omega_2 t \tag{2-5}$$

,  $y(t)$

가

$$\alpha_2 A_1 A_2 \cos (\omega_1 - \omega_2) t \tag{2-6}$$

$$\cos \omega_{LO} t \tag{2-6}$$

RF-IF

가

가

RF

IF

가

AM

가

fading

$$, x_{in}(t) = (A + c \cos \omega_m t) (a \cos \omega_c t + b \sin \omega_c t) \text{가}$$

$$(c \cos \omega_m t : ) \tag{2-7}$$

$(a^2 + b^2)A^2 c \cos \omega_m t$  .  $(a^2 + b^2)A^2 c \cos \omega_m t$   
 even-order distortion demodulator AM

component , .

가 , 가 , .

$\frac{1}{2}$  ,  $\frac{1}{2}$  , LO  
 $\frac{1}{2}$  , .

, RF LO

RF 가 , 가 , .

$\frac{1}{2}$  IP2 (Second Intercept Point) .

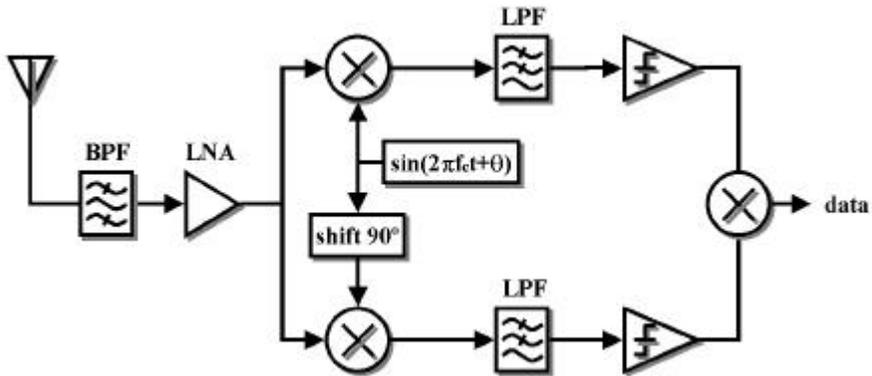
bit . plot IP2

, 가 , .  
 duplexer single-ended  
 single-ended . ,

가 , noise figure  
 single-ended .

### 2-3. Direct-Conversion

900 MHz ISM



2- 12 Direct- conversion

Fig. 2- 12 Direct-Conversion Receiver Block-Diagram.

2-3

2-3

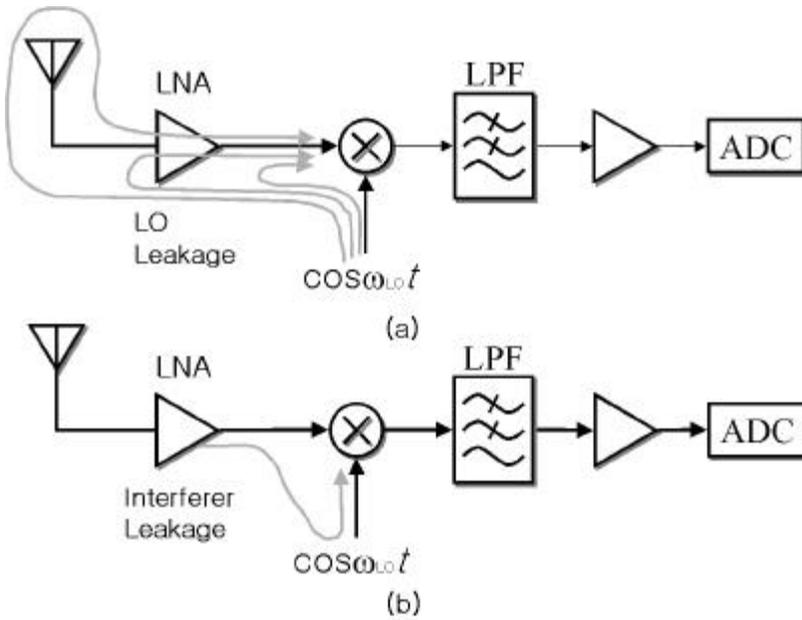
Table 2-3 Design Parameter.

Data rate	32 kbps
	QPSK
	FDD
	915-928 MHz
	10 mW
	50 kHz
	$20 \times 10^{-6}$

(32Kbps)  
900MHz ISM band  
QPSK  
AWGN 가  
-60 dBm  
RF isolation -40 dBm

3-1. DC-offset

DC-offset Heterodyne ,  
 Direct-conversion . DC-offset  
 Offset voltage ,  
 DC-offset



3-1 Self-mixing (a) (b) LO

Fig. 3- 1 Self-mixing of (a) Interferers. (b) LO.

DC-offset 가 가 .  
 (Local Oscillator) RF Port , isolation  
 , DC-offset 3-1

가  
 3-1(a)

LO  
 Self-mixing  
 Heterodyne  
 offset  
 가  
 dc  
 DC-offset  
 DC-offset

LO-Leakage  
 ,  
 ,  
 dc  
 Self-mixing  
 ,  
 Self-mixing  
 DC-offset  
 DC-offset  
 Isolation

가  
 가  
 DC-offset  
 Direct-conversion  
 DC-offset  
 DC-offset

DC-offset  
 ,  
 가 , 가

DC-offset

AC-Coupling

DC-offset

AC-coupling

DC-offset

AC-coupling

DC-feedback loop

4

, DC-offset

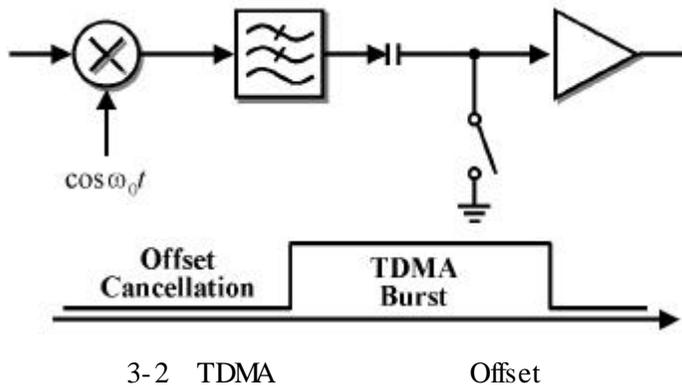


Fig. 3-2 Offset cancellation in a TDMA system.

(Idle)

3-2

TDMA

DC-offset

DC-offset

3-2

$S_1$

C가

DC-free coding

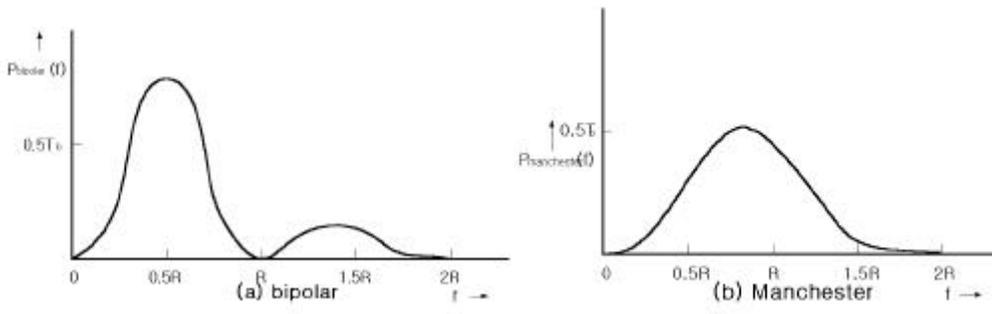
DC-offset

source coding

dc

coding

Manchester NRZ



3-3 Code PSD (a) bipolar NRZ, (b) Manchester NRZ

Fig. 3-3 PSD for line codes (a) bipolar NRZ. (b) Manchester NRZ.



DC-offset

가

Isolation 가

LO 가

, LO

DC-offset

(  $\delta_{dsr}^3$  ). 3-4 DC-offset

$$\xi_{dsr}^3 = \frac{P_{dco}^3}{P_{usr}^3} = \frac{P_{lo} I_{lo}^1 (1 + \alpha) G_{lna}/2 + P_{lo} I_{lo}^2}{P_{usr}^1 G_{lna}} \quad (3-1)$$

$\xi_{dsr}^3$  60 80 dB 가

[1] DC-offset

DC-offset

DC-offset

, DC-offset

가

가

, Doppler

가

. Doppler

LO

가

DC

, ,

가

DC-offset

Doppler

가

가

가

가

, 가

가 가

가 C 가  
Doppler

$$\Delta f = \frac{2vf \cos \theta}{C} = \frac{2vf}{C} \quad (3-2)$$

900 MHz 200  
Km/h Doppler shift frequency 166 Hz

DC-offset , DC-offset  
LO RF ( $I_{lo}^2$ ), LNA ( $I_{lo}^1/2$ ),  
( $\alpha I_{lo}^1/2$ ) . 3-4 DCR DC-offset  
 .  $\alpha$  ,  
 가

LNA .  
가 LO leakage . , , -  
 .[2] LO RF Self-mixing  
 , dc . Self-mixing  
 AGC setting .  
 DC-offset

가 DC-offset DC-offset  
 , DC-offset

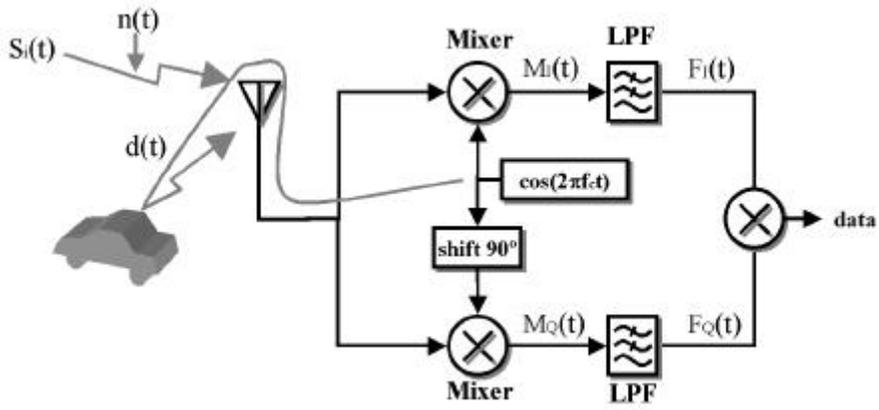
3-4  
 . Dynamic offset  
 $\alpha I_{lo}^1 P_{lo} G_{lna} G_{mix}/2$  . offset

(  $\xi^3_{ddsr}$  ) .

$$\xi^3_{ddsr} = \frac{\alpha I^1_{lo}}{2} \frac{P_{lo}}{P^1_{usr}} \quad (3-3)$$

### 3-3. AWGN

DC-offset 가  
 Doppler shift DC-offset . Doppler shift  
 DC-offset AWGN  
 Modeling .



3-5 Doppler Shift DC-offset

Fig. 3-5 Environment of time variant DC-offset by Doppler shift

3-5 DC-offset . 3-5

$$s_i(t) = \frac{A}{\sqrt{2}} [a_i \cos 2\pi f_c t - b_i \sin 2\pi f_c t], \quad n(t)$$

,  $d(t) = \beta B \cos(2\pi f_c t - 2\pi f_d t)$  Doppler shift

,  $\beta$  mismatch

, B, LO  $\cos(2\pi f_c t)$  .

$$s_i(t) \quad n(t),$$

$$d(t)$$

$$\begin{aligned}
r(t) &= s_i(t) + n(t) + d(t) \\
&= \frac{A}{\sqrt{2}} [a_i \cos 2\pi f_c t - b_i \sin 2\pi f_c t] \\
&\quad + n(t) + \beta B \cos (2\pi f_c t - 2\pi f_d t)
\end{aligned} \tag{3-4}$$

QPSK, I, Q  
가, I.

$$\begin{aligned}
M_I(t) &= \frac{A}{\sqrt{2}} [a_i \cos 2\pi f_c t - b_i \sin 2\pi f_c t] \cos (2\pi f_c t) \\
&\quad + n(t) \cos (2\pi f_c t) + \beta B \cos (2\pi f_c t - 2\pi f_d t) \cos (2\pi f_c t)
\end{aligned} \tag{3-5}$$

$$\begin{aligned}
F_I(t) &= \frac{1}{T} \int_0^T \frac{A}{\sqrt{2}} [a_i \cos 2\pi f_c t] dt \\
&\quad - \frac{1}{T} \int_0^T \frac{A}{\sqrt{2}} [b_i \sin 2\pi f_c t \cos (2\pi f_c t)] dt \\
&\quad + \frac{1}{T} \int_0^T n(t) \cos (2\pi f_c t) dt \\
&\quad + \frac{1}{T} \int_0^T \beta B \cos (2\pi f_c t - 2\pi f_d t) \cos (2\pi f_c t) dt
\end{aligned} \tag{3-6}$$

$$F_I(t) = a_i \frac{A}{2\sqrt{2}} + N_1 + D_1 \tag{3-7}$$

$$N_1 = \frac{1}{T} \int_0^T n(t) \cos (2\pi f_c t) dt$$

$$D_1 = \frac{B}{T} \int_0^T \beta \cos (2\pi f_c t - 2\pi f_d t) \cos (2\pi f_c t) dt$$

Q

$$F_{\varrho}(t) = b_i \frac{A}{2\sqrt{2}} + N_2 + D_2 \quad (3-8)$$

$$N_2 = \frac{1}{T} \int_0^T n(t) \sin(2\pi f_c t) dt$$

$$D_2 = \frac{B}{T} \int_0^T \beta \cos(2\pi f_c t - 2\pi f_d t) \sin(2\pi f_c t) dt$$

, gaussian  $N_1, N_2$ ,

Doppler shift DC-offset

.  $D_1, D_2$  .

$$\sigma_1^2 = E \{ (N_1 + D_1)^2 \} = E \{ (N_1^2 + 2N_1 D_1 + D_1^2) \} \quad (3-9)$$

$$\begin{aligned} \sigma_n^2 &= E \{ N_1^2 \} = E \left\{ \left[ \int_0^T n(t) \cos(2\pi f_c t) dt \right]^2 \right\} \\ &= \int_0^T \int_0^T E \{ n(t) n(\alpha) \} \cos(2\pi f_c t) \cos(2\pi f_c \alpha) d\alpha dt \\ &= \int_0^T \int_0^T \frac{N_0}{2} \delta(t - \alpha) \cos(2\pi f_c t) \cos(2\pi f_c \alpha) d\alpha dt \\ &= \frac{N_0}{2} \int_0^T \cos^2 2\pi f_c t dt \\ &= \frac{N_0 T}{4} \end{aligned} \quad (3-9-1)$$

$$\begin{aligned} \sigma_d^2 &= E \{ D_1^2 \} = E \left\{ \left[ \int_0^T \beta \cos(2\pi f_c t - 2\pi f_d t) \cos(2\pi f_c t) dt \right]^2 \right\} \\ &= \int_0^T \int_0^T [ \beta \cos(2\pi f_c t - 2\pi f_d t) \cos(2\pi f_c t) ] \\ &\quad \cdot [ \beta \cos(2\pi f_c \alpha - 2\pi f_d \alpha) \cos(2\pi f_c \alpha) ] d\alpha dt \\ &= \beta^2 \int_0^T \cos^2(2\pi f_c t - 2\pi f_d t) \cos^2(2\pi f_c t) dt \\ &= \beta^2 \int_0^T \left[ \frac{1}{2} + \frac{\cos(4\pi f_c t - 4\pi f_d t)}{2} \right] \left[ \frac{1}{2} + \frac{\cos 4\pi f_c t}{2} \right] dt \\ &= \frac{\beta^2}{4} \int_0^T (1 + 2 \cos(4\pi f_c t - 4\pi f_d t) \cos 4\pi f_c t + \cos^2 4\pi f_c t) dt \\ &= \frac{\beta^2 T}{4} \end{aligned} \quad (3-9-2)$$

$$E \{2N_1 D_2\} = 2\beta \int_0^T \int_0^T E \{n(t)\} \cos(2\pi f_c t) \cdot \cos\{2\pi(f_c - f_d)\alpha\} d\alpha dt = 0 \quad (3-9-3)$$

I

$$\sigma_1^2 = \frac{(N_o + \beta^2)T}{4} \quad (3-10)$$

$s_i(t)$  가 I Q BPSK

$$P_1(e) = P_2(e) = \frac{1}{2} \operatorname{erfc} \left[ \sqrt{\frac{E_s}{2(N_o + \beta^2)}} \right] \quad (3-11)$$

$$T = 2T_b \quad E_s = 2E_b$$

$P_e$

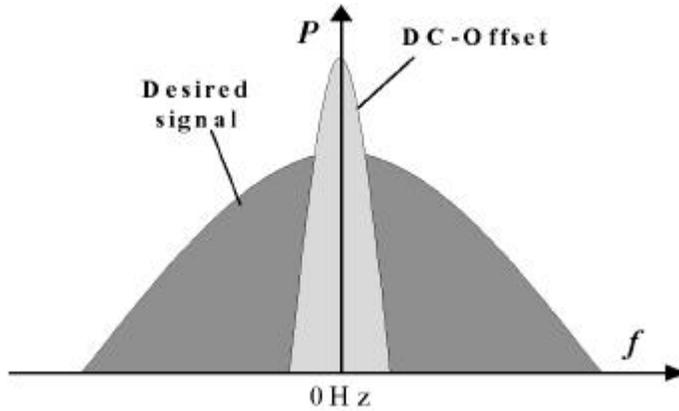
$$\begin{aligned} P(e) &= 1 - P_c \\ &= 1 - [1 - P_1^2(e)]^2 = 2P_1(e) - 2P_1^2(e) \\ &= \frac{1}{2} \operatorname{erfc} \left[ \sqrt{\frac{E_s}{2(N_o + \beta^2)}} \right] \end{aligned} \quad (3-12)$$

$$\frac{E_s}{N_o + \beta^2} \gg 1$$

$$P(e) \approx \operatorname{erfc} \left[ \sqrt{\frac{E_s}{2(N_o + \beta^2)}} \right] = \operatorname{erfc} \left[ \sqrt{\frac{E_b}{N_o + \beta^2}} \right] \quad (3-13)$$

## 4 DC-offset

DC-offset



4- 1 spectrum DC- offset

Fig. 4- 1 DC- offset on the baseband spectrum.

AC-coupling

. AC-coupling

DC-offset

가 ,

DC-offset

AC-coupling 가

DC-offset

가 . ,

DC-offset

, dc

Direct-Conversion

BER

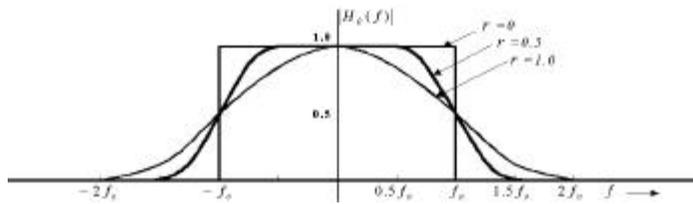
가 . ,

, AC-coupling  
 AC-coupling

4-1.

$$H_e(f) = \begin{cases} 1, & |f| < f_1 \\ \frac{1}{2} \left\{ 1 + \cos \left[ \frac{\pi(|f| - f_1)}{2f_\Delta} \right] \right\}, & |f| < B \\ 0, & |f| > B \end{cases} \quad (4-1)$$

$$h_e(t) = \mathcal{F}^{-1}[H_e(f)] = 2f_0 \left( \frac{\sin 2\pi f_0 t}{2\pi f_0 t} \right) \left[ \frac{\cos 2\pi f_0 t}{1 - (4f_0 t)^2} \right] \quad (4-2)$$



4-2 rolloff factor

Fig. 4-2 Magnitude frequency response for different rolloff factor.

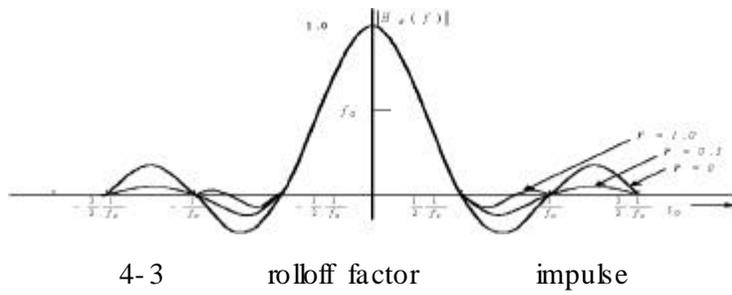


Fig. 4-3 Impulse(time) response for different rolloff factor.

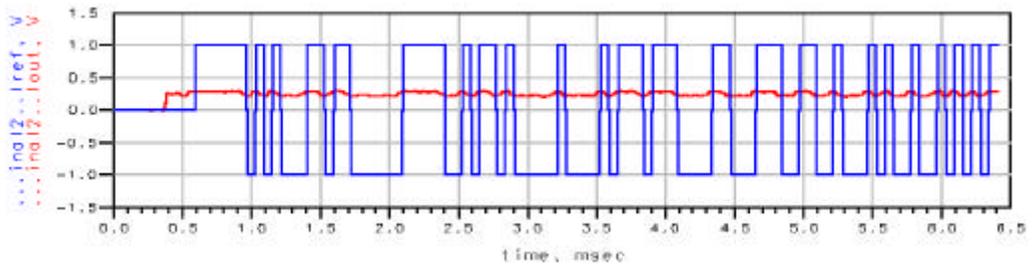
ISI(Intersymbol Interference)

Raised-cosine-filter , Roll-off

0.5 .

## 4-2. AC-Coupling

DC-offset 가 ,  
 DC-offset 100 Hz 가 ,  
 100 Hz DC-offset  
 40 60 dB  
 , Direct-Conversion DC-offset  
 AC-coupling AC-coupling  
 AC-coupling  
 100 Hz 가 ,



4-4

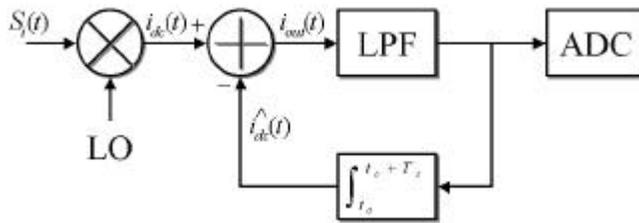
Fig 4-4 Waveform of Input and Output signal in baseband.

가 , 5  
 Butterworth

### 4-3. DC-Feedback

### DC-offset

AC-coupling      dc  
 BER      ,      Feedback  
 ,      dc  
 coupling      DC-offset



4-5      Coupling      DC- offset

Fig. 4-5 DC- offset occur coupling with reference signal.

$$S_i(t) = \frac{A}{\sqrt{2}} \cos [2\pi f_c t + \Phi_i(t)] + n(t) + R_{dc} \cos (2\pi f_c t + \Phi_{dc}) \quad (4-3)$$

,  $\Phi_i(t)$

$R_{dc}$

$\phi_{dc}$       (0 2      )

$$S_i(t) = A_s \cos [2\pi f_c t + \phi(t) + \eta(t)] + A_{dc} \cos (2\pi f_c t + \phi_{dc}) \quad (4-4)$$

,  $A_s$

$\phi(t)$  ISI

$\eta(t)$  가

$$d(t) = \phi(t) \quad .$$

(The directly converted in-phase and quadrature  
-phase component)

$$i_{dc}(t) = A_s \cos [\phi(t) + \eta(t)] + A_{dc} \cos (\phi_{dc}) \quad (4-5a)$$

$$q_{dc}(t) = A_s \sin [\phi(t) + \eta(t)] + A_{dc} \sin (\phi_{dc}) \quad (4-5b)$$

dc

$$\hat{i}(t) \quad \hat{q}(t)$$

$$i_{dc}(t) \quad q_{dc}(t)$$

Feedback

$$\int_{t_o}^{t_o+T_s} \cos (\theta(t)) dt = \int_{\theta_o}^{\theta_o+2n\pi} \cos \theta = 0 \quad (4-6a)$$

$$\int_{t_o}^{t_o+T_s} \sin (\theta(t)) dt = \int_{\theta_o}^{\theta_o+2n\pi} \sin \theta = 0 \quad (4-6b)$$

$$\int_{t_o}^{t_o+T_s} A_s \cos (\theta(t) + \eta(t)) dt \approx 0.0 \quad (4-7a)$$

$$\int_{t_o}^{t_o+T_s} A_s \sin (\theta(t) + \eta(t)) dt \approx 0.0 \quad (4-7b)$$

가

$$\begin{aligned}
i_{out}(t) &= i_{dc}(t) - \widehat{i_{dc}}(t) \\
&= A_s \cos[\phi(t) - \eta(t)] + A_{dc} \cos(\phi_{dc}) - \int_0^{T_s} A_{dc} \cos(\phi_{dc}) dt
\end{aligned} \tag{4-8}$$

coupling

$\phi_{dc}$

$$i_{dc} = A_s \cos[\phi(t) - \eta(t)] + \theta_{dc} \tag{4-9}$$

$\theta_{dc}$  DC-offset

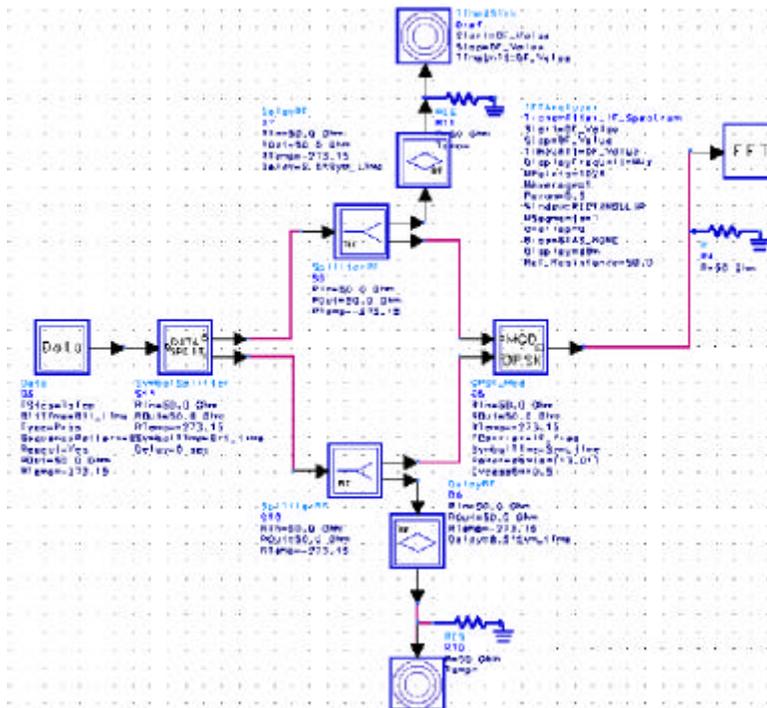
$\theta \approx 0$

$$i_{out} = A_s \cos[\phi(t) - \eta(t)] \tag{4-10}$$

가

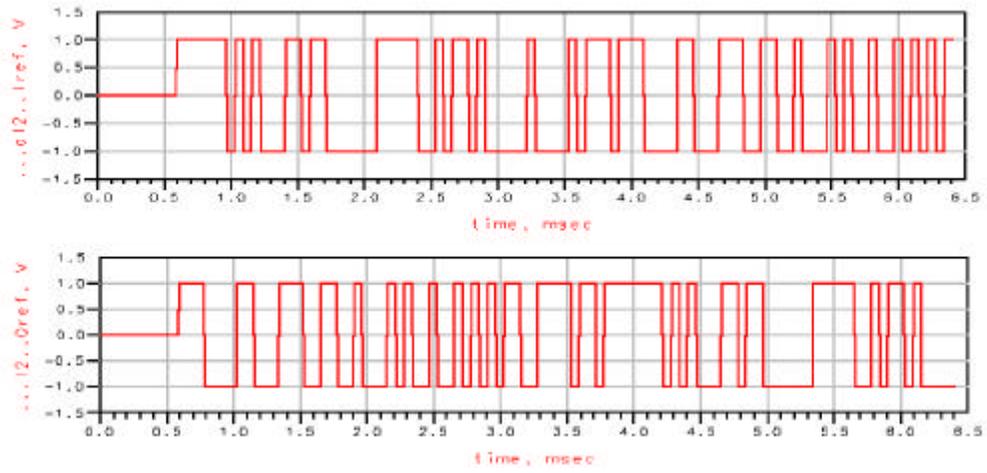
5-1. QPSK

5-1-1 QPSK



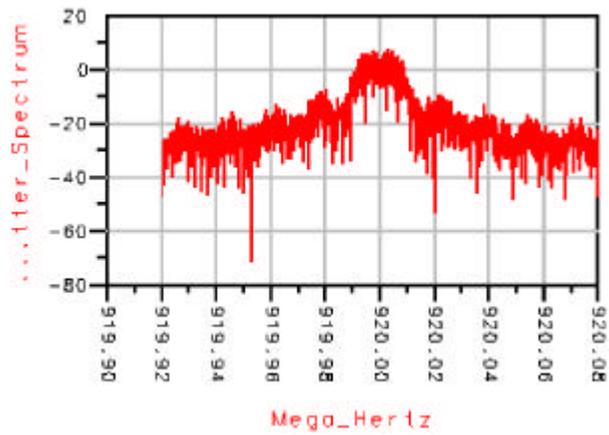
5- 1

Fig. 5- 1 Transmitter.



±x 5-2 I Q

Fig. 5-2 Input data of I, Q channel.

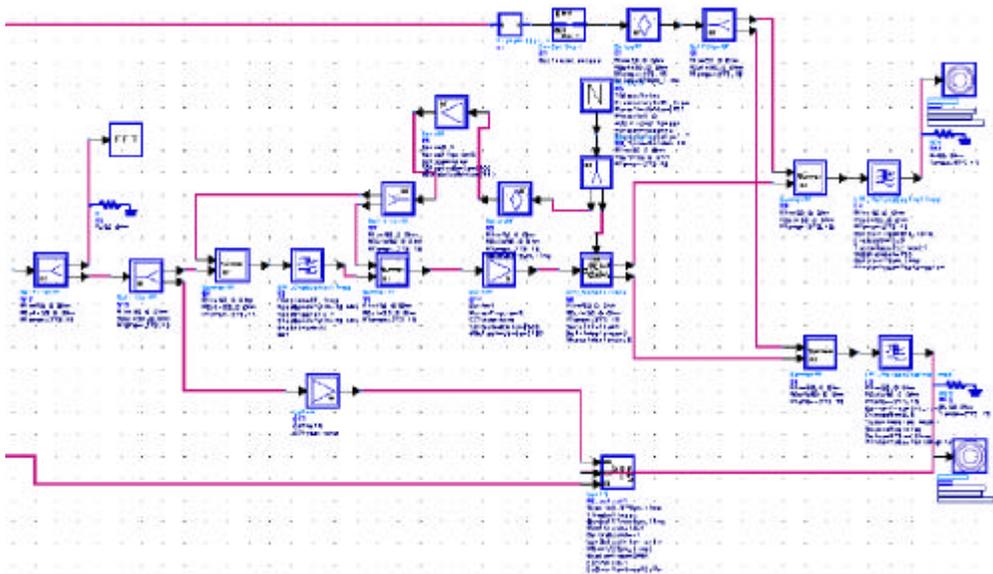


5-3 Spectrum

Fig. 5-3 Spectrum of transmitter.

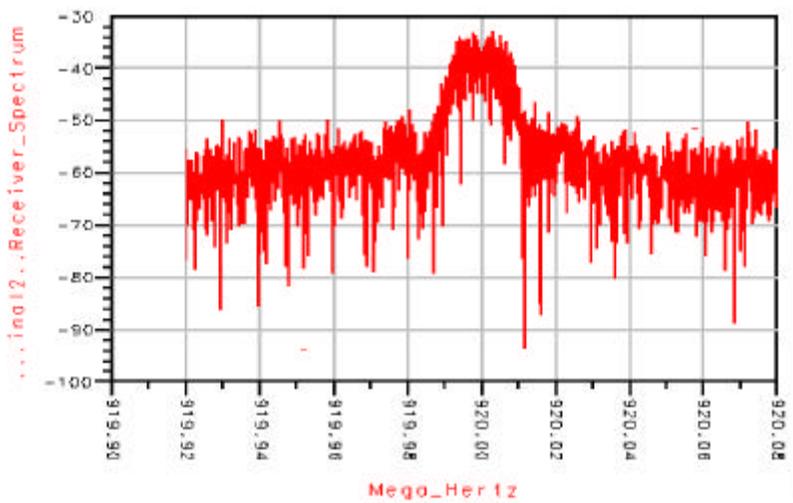


5-2-2



5-5

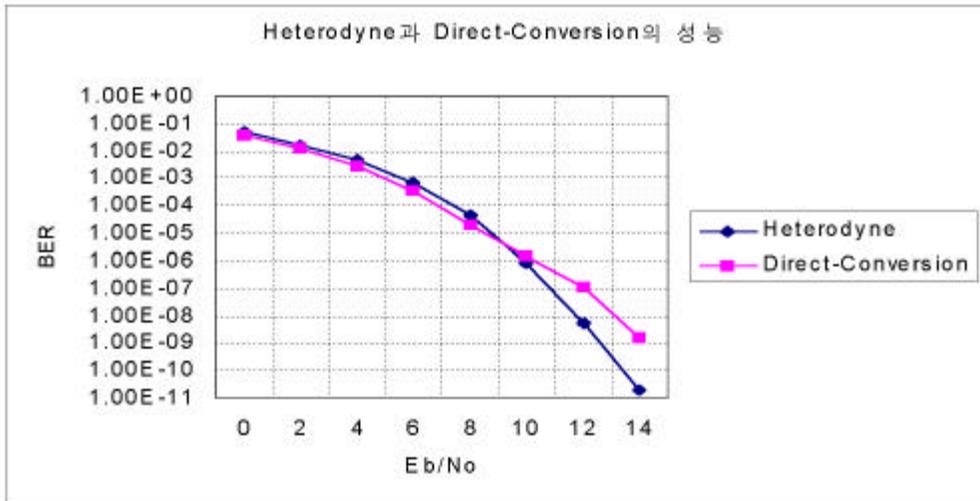
Fig. 5-5 Receiver Design.



5-6 Spectrum

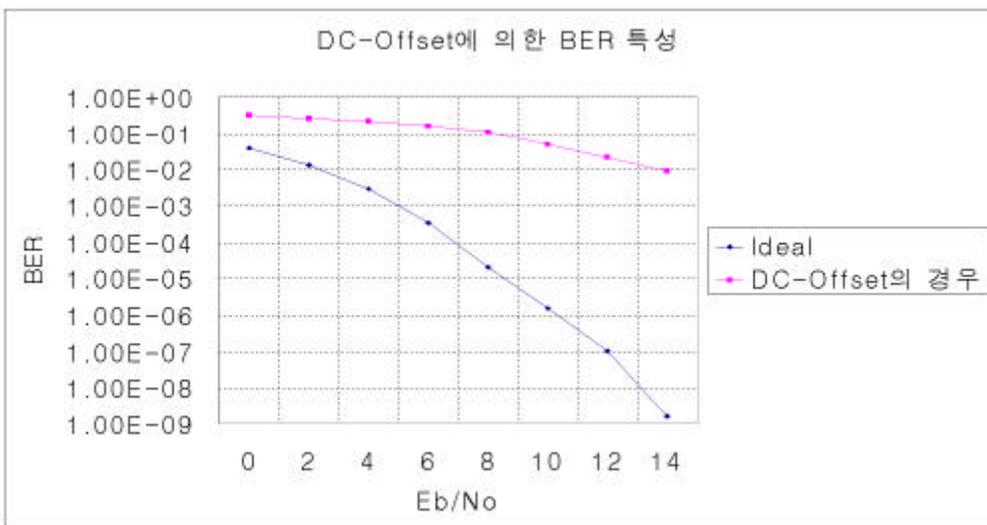
Fig. 5-6 Spectrum of Receiver.

5-3.



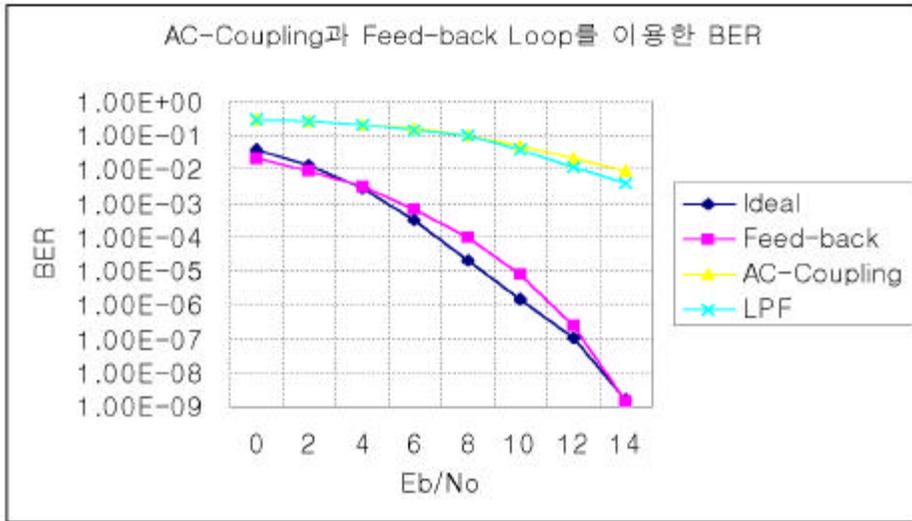
5-7 Heterodyne Direct-Conversion BER

Fig. 5-7 BER of Heterodyne and Direct-Conversion.



5-8 DC-offset BER

Fig. 5-8 Character of BER in DC-offset.



5-9 AC-coupling      Feed-back Loop      BER

Fig. 5-9 BER in the case of Adopting AC-coupling and Feed-back Loop.

6

가 IMT-2000

가

Direct-conversion

Direct-conversion

DC-offset

가

가

Direct-conversion

DC-offset

AC-coupling

가 DC-offset

가

AC-coupling

DC-offset

0.5 V

DC

가

dc

10 dB

2 dB

BER

dc

feedback

32 kbps

coupling

$10^{-5}$  , 2 dB  
, AC-coupling ,  
Direct-conversion  
, DC-offset  
feedback , feedback  
DC-offset

- [1] TGS RAN Working Group (Radio), R4-99024, 3GPP TSG RAN WG4 S4.01Av0.01(1999-02), UTRA(UE)FDD ; Radio Transmission and Reception, Feb. 1999.
- [2] Behzad Razavi, "Design Considerations for Direct-Conversion Receivers," IEEE Trans. on Circuits and Systems- , Vol. 44, pp. 428-435, Jun. 1997.
- [3] A. A. Abidi, "Direct-Conversion radio trnsceivers for digital communications," IEEE J. Solid-State Circuits, Vol. 30, pp. 1399-1410, Dec. 1995.
- [4] Bing Wang, Hyuck M. Kwon, and Jim Mittel, "Simple DC Removers for Digital FM Direct-Conversion Receiver," Proceedings of the 49th Vehicular Technology Conference - Volume 2, pp. 1222-1226, May 1999.
- [5] Young Sun Kim, Seung-Geun Kim, and Kiseon Kim, "BER Performance of Frequency Estimators in Burst-mode QPSK Transmissions," Proceedings of ITC-CSCC, pp. 1290-1293, 1999.
- [6] Bernard Skalar, Digital Communications Fundamentals and Applications, Prentice Hall, 1988.

2

,

1

,

.

,

.

,

,

,

. 가

..

가

,

,

,

,

,

,

,

,

.

,

,

.

,

,

,

,

,

,

,

,

,

,

,

.

,

,

.